

Retraction

Retracted: A New Method of Denoising Crop Image Based on Improved SVD in Wavelet Domain

Security and Communication Networks

Received 26 December 2023; Accepted 26 December 2023; Published 29 December 2023

Copyright © 2023 Security and Communication Networks. This is an open access article distributed under the Creative Commons Attribution License, which permits unrestricted use, distribution, and reproduction in any medium, provided the original work is properly cited.

This article has been retracted by Hindawi, as publisher, following an investigation undertaken by the publisher [1]. This investigation has uncovered evidence of systematic manipulation of the publication and peer-review process. We cannot, therefore, vouch for the reliability or integrity of this article.

Please note that this notice is intended solely to alert readers that the peer-review process of this article has been compromised.

Wiley and Hindawi regret that the usual quality checks did not identify these issues before publication and have since put additional measures in place to safeguard research integrity.

We wish to credit our Research Integrity and Research Publishing teams and anonymous and named external researchers and research integrity experts for contributing to this investigation.

The corresponding author, as the representative of all authors, has been given the opportunity to register their agreement or disagreement to this retraction. We have kept a record of any response received.

References

- [1] R. Wang, W. Cai, and Z. Wang, "A New Method of Denoising Crop Image Based on Improved SVD in Wavelet Domain," *Security and Communication Networks*, vol. 2021, Article ID 9995813, 11 pages, 2021.

Research Article

A New Method of Denoising Crop Image Based on Improved SVD in Wavelet Domain

Rui Wang,¹ Wanxiong Cai²,³ and Zaitang Wang^{3,4}

¹Technology School, Jilin Business and Technology College, Changchun 130021, Jilin, China

²Department of Electrical Engineering, Guangxi Technological College of Machinery and Electricity, Nanning 530007, Guangxi, China

³School of Public Economics and Administration, Shanghai University of Finance and Economics, Shanghai 200433, China

⁴School of Taxation, Jilin University of Finance and Economics, Changchun 130021, Jilin, China

Correspondence should be addressed to Wanxiong Cai; wanxch83@gmail.com

Received 4 March 2021; Revised 21 March 2021; Accepted 4 July 2021; Published 26 August 2021

Academic Editor: Chi-Hua Chen

Copyright © 2021 Rui Wang et al. This is an open access article distributed under the Creative Commons Attribution License, which permits unrestricted use, distribution, and reproduction in any medium, provided the original work is properly cited.

In real life, images are inevitably interfered by various noises during acquisition and transmission, resulting in a significant reduction in image quality. The process of solving this kind of problem is called image denoising. Image denoising is a basic problem in the field of computer vision and image processing, which is essential for subsequent image processing and applications. It can ensure that people can obtain more effective information of images more accurately. This paper mainly studies a new method of crop image denoising with improved SVD in wavelet domain. The algorithm used in this study firstly carried out a 3-layer wavelet transform on the crop noise image, leaving the low-frequency subimage unchanged; then, for the high-frequency subimages distributed in the horizontal, vertical, and diagonal directions, the improved adaptive SVD algorithm was used to filter the noise; finally perform wavelet coefficient reconstruction. To effectively test the performance of the algorithm, field crop images were taken as test images, and the denoising performance of the algorithm, SVD algorithm, and the improved SVD algorithm used in this study were compared, and the peak signal-to-noise ratio (PSNR) was introduced. Quantitative evaluation of the denoising results of several types of algorithms. The experimental data in this paper show that when the noise standard deviation is greater than 20, the enhanced experimental results clearly achieve higher PSNR and SSIM values than WNNM. The average peak signal-to-noise ratio (PSNR) is about 0.1 dB higher, and the average SSIM is larger about 0.01. The results show that the algorithm used in this study is superior to the other two algorithms, which provides a more effective method for crop noise image processing.

1. Introduction

1.1. Background Significance and Innovation. In the recent years, with the continuous development and application of various computer networks and multimedia technologies, the role of information has become increasingly important. Among them, about 80% of the information is the visual information that people obtain from the outside world, and the image is the most intuitive and vivid visual information. This makes the image as a medium, and it has become an indispensable and important tool in human life. It can help mankind to better understand the world and at the same time provides a key basis for mankind to make correct decisions. However, in reality, any image will be interfered

by various factors such as the external environment, dust, and sensitivity of sensitive components during the acquisition and transmission process, which causes a lot of noise in the original image, which seriously reduces the image visual effect has an adverse effect on further analysis and processing (such as pattern recognition, 3D reconstruction, feature extraction, and texture analysis). Therefore, using appropriate methods to remove or reduce these noises is an essential preprocessing step, and it is one of the most basic and important tasks in the field of agricultural informatization and automation research. The key problem in image processing is to identify the information required for interference and recovery. There are many types of interference. According to the image characteristics and

interference distribution, researchers have proposed various forms of denoising methods. Image denoising is an objective process. The goal is to filter out noise and increase the peak signal-to-noise ratio (PSNR) on the basis of not losing the original information as much as possible. The final purpose of denoising is to solve the problem of image quality degradation caused by noise interference. It is an important preprocessing method that lays a good foundation for the subsequent digital image processing. The noise in the image is often interwoven with the signal.

Therefore, how to remove the noise in the point image and keep the image content as much as possible is the main problem of the image denoising process. The ultimate goal of image denoising is to effectively remove the noise while retaining important image features and details as much as possible without generating false texture information. To achieve this goal, researchers have proposed various effective denoising methods. However, because noise, edges, and textures are high-frequency information, it is difficult to distinguish them during the denoising process. With the in-depth development of computer network technology and computer graphics and image processing technology, it is increasingly applied in the field of agriculture, greatly improving the degree of agricultural informatization and intelligence, monitoring crop growth in real time, and accurately formulating crop fertilization scheme. With the rapid popularization of Internet in China, the attack on China's information system also presents a rapid growth trend. The essence of computer network security is to prevent network attacks and ensure system security. The antiattack method is the analysis of the attack flow from the source, and then the defense is carried out according to the attack method and type; then the study of computer network security protection is the study of the attack flow. The improved SVD wavelet domain crop image denoising used in this paper also relies on the computer network. Therefore, more attention should be paid to network security communications.

For agricultural disease image recognition, the obtained image is usually not clear, which may lead to poor recognition effect in the actual production environment. Image quality has an important influence on the recognition accuracy of the pretrained image classifier. To solve this problem, we propose a generative confrontation network with dual attention and topology fusion mechanism, called DATFGAN. The network can effectively convert unclear images into clear, high-resolution images. In addition, the weight sharing scheme in our proposed network can significantly reduce the number of parameters. Experimental results show that DATFGAN has better visual effects than the most advanced methods. In addition, the processed image is evaluated according to the recognition task. The results show that the proposed method is significantly better than other methods and has sufficient robustness for practical use [1].

The innovation of this paper: (1) This paper studies a denoising algorithm of crop image based on hybrid wavelet transform and applies it to crop images. According to the theory of heterosis, the two images processed by wavelet

adaptive threshold denoising and Wiener filtering are coded to form a population with a certain number of individuals, which are called paternal and maternal. The operation of hybridization and mutation, with the hope that the final population after hybridization is decoded and reduced to an image, can show better characteristics than its parents. (2) This paper studies the difference of using wavelet adaptive threshold denoising under different wavelet bases and the main reasons for these differences. According to the results of the study, an optimal wavelet base is selected for the father of the hybrid wavelet denoising algorithm.

1.2. A Literature Review. According to the theory of deep learning, Y. Lü believes that the image denoising process can be regarded as a neural network fitting process. By constructing a simple and effective compound convolutional neural network, an image denoising algorithm based on the compound convolutional neural network is proposed. The first stage consists of two convolutional neural networks with two layers. In the second stage, some initial convolution kernels on a three-layer convolutional neural network are trained by these two networks, respectively. The training time of the second stage is reduced, and the robustness of the network is enhanced. Finally, the convolutional neural network learned in the second stage is used to denoise new images with noise. Experimental results show that the algorithm is comparable to existing image denoising algorithms in terms of peak signal-to-noise ratio (PNSR), structural similarity, and root mean square error (RMSE). Especially when the noise becomes larger, the algorithm performs better with less training time [2]. Li Jian determines the Gaussian standard deviation by calculating the ratio of the variance of the center point neighborhood in the image pixel matrix area to the two-dimensional Gaussian filter function and dynamically generates the Gaussian convolution kernel, thereby forming an improved adaptive Gaussian filtering algorithm, denoising and smoothing the diseased image, and then simulating different noise intensities and comparing the denoising effects of the algorithms. [3]. Li Jianglong believes that with the rapid development of computer visualization technology and Internet technology, traditional agricultural management methods are gradually being replaced by new agricultural information management methods. At present, smart agriculture based on digital image processing technology has become a new type of agricultural informatization in the key research area, a semireference quality evaluation method based on visual saliency is proposed, and the directional histogram features are extracted in the gradient domain to describe the changes in image quality [4].

Experts also have a lot of research on crop image deirritation, Vargas believes that traditional crop lodging assessment methods require accurate ground observations and are often laborious. Therefore, remote sensing data from small unmanned aerial systems (UAS) and low-orbit satellites (LOS) can be used to improve accommodation evaluation methods and accuracy. Extract the crop surface model (CSM) and six image color features from

small UAS-based data. Then these features are divided into non-embedded (NL), partially embedded (PL), and embedded (L) groups. The average and majority feature classes of the region of interest are obtained [5]. Dai believes that for agricultural disease image recognition, the obtained image is usually not clear, which will lead to poor recognition in the actual production environment. Image quality has a significant impact on the recognition accuracy of the pretrained image classifier. The weight sharing scheme in the proposed network can significantly reduce the number of parameters. Experimental results show that DATFGAN produces more pleasing results compared to the state-of-the-art methods. In addition, the processed images are evaluated according to the recognition task. The results show that the proposed method is significantly better than other methods and is robust enough for practical use [6]. These studies provide a lot of reference for the crop image demanipulation in this article, but because the sample size of these studies is too small, they are only of reference value.

2. Proposed Method

2.1. Image Denoising Method. The image will be interfered by various factors and generate noise during the actual acquisition and transmission process. There are various methods of noise classification. According to the fusion method between noise and image information, the noise model can be divided into two types: additive noise model and multiplicative noise model [5–7].

The additive noise model is to superimpose a random noise signal on the ideal noise-free image, and the intensity of the noise signal and the image signal are not related. The mathematical model can be expressed as follows:

$$g(x, y) = f(x, y) + \eta(x, y), \quad (1)$$

where $g(x, y)$ is a noise-contaminated image signal, $f(x, y)$ is an original noise-free image signal, and $\eta(x, y)$ is a noise signal.

The multiplicative noise model is closely related to the image signal, and its noise term is often modulated by the image signal. The mathematical model of this type of noise can be expressed as follows:

$$g(x, y) = f(x, y) + f(x, y)\eta(x, y), \quad (2)$$

where $g(x, y)$ is a noise-contaminated image signal, $f(x, y)$ is an original noise-free image signal, and $\eta(x, y)$ is a noise signal.

It can be seen that the noise signal is changed by the change of the original image signal. Usually, the signal changes very little, and the second term can be approximately unchanged. At this time, the multiplicative noise degenerates into additive noise. Generally, the noise that affects the image quality is mostly additive noise, and the multiplicative noise can also be converted into additive noise in some ways. Therefore, most of the noise models under study are additive noise, and it can be approximated as Gaussian noise.

2.2. Image Denoising Algorithm. Singular value decomposition (SVD) is a new type of nonlinear filtering algorithm. From the perspective of the image matrix, the image is singularly decomposed and the matrix vector corresponding to the larger singular value is selected for reconstruction. Noise filtering: This research draws on the current theme research ideas in this field and combines it with wavelet transform on the basis of appropriate improvements to SVD to achieve effective processing of crop noise images. Theoretical analysis and experimental results show that the performance of the algorithm used in this study is superior to SVD and the improved SVD algorithm [8].

After the noisy image $Y \in R^{n \times m}$ is transformed by SVD, the main feature information of the image is concentrated on the singular value. A natural method to obtain the estimated data from the noisy data is to truncate the singular value of the observation matrix Y , which is hard threshold processing, or the singular values of the observation matrix Y are soft thresholded.

Let $g: R^{n \times m} \rightarrow R^{n \times m}$ be the matrix recovery function,

$$Y = U \sum V^T = \sum_{i=1}^{\min(n,m)} \lambda_i u_i v_i^T, \quad (3)$$

where $u_i \in R^n, v_i \in R^m, i = 1, \dots, \min(n, m)$ is the left-right singular vector corresponding to the singular value in Y , $\sum = \text{diag}(\lambda_1, \lambda_2, \dots, \lambda_k)$, and $k = \min(n, m)$.

Then the hard threshold processing method for singular values is

$$g_\tau^H(Y) = \sum_{i=1}^{\min(n,m)} \lambda_i 1(\lambda_i \geq \tau) u_i v_i^T. \quad (4)$$

Among them is the $1(\bullet)$ indicator function, $\tau > 0$ is the threshold parameter that constrains the singular value, and the indicator function takes the following values:

$$1(\bullet) = \begin{cases} 1, & \lambda_i \geq \tau, \\ 0, & \text{otherwise.} \end{cases} \quad (5)$$

Among them, $(x_+) = \max(x, 0)$. After processing the singular value through the hard (soft) threshold, the estimated $\hat{\lambda}_i$ and $\sum \text{diag}(\hat{\lambda}_1, \hat{\lambda}_2, \dots, \hat{\lambda}_k)$ are obtained, and then the inverse SVD transformation is performed:

$$\hat{Y} = U \sum V^T = \sum_{i=1}^{\min(n,m)} \hat{\lambda}_i u_i v_i^T. \quad (6)$$

You can get an estimate of the entire image.

In the above two singular value threshold (SVT) estimation operations, the threshold τ is approximately 0, and clearly a lot of information will be missing, resulting in the image information not getting a good estimate, through adaptive selection of the threshold, that is, the singular values of different a are constrained by different thresholds, which can improve this problem. By choosing different thresholds for different singular values to shrink, it will not only retain as much image information as possible but also play a good denoising effect [9]. Specific steps are as follows:

Step 1: Divide the image into blocks of $\sqrt{n} \times \sqrt{n}$ size, generally 8×8 , and step size k generally 3.

Step 2: For each small block $l(i: i + \sqrt{n} - 1, j: j + \sqrt{n} - 1)$, use the nonlocal similarity block measurement method to find m similar blocks, arrange the similar blocks into a matrix Y in the form of columns, and perform SVD decomposition on the matrix:

$$Y = U \begin{pmatrix} \sum & 0 \\ 0 & 0 \end{pmatrix} V^T, \quad (7)$$

where U and V are the orthogonal matrices of $m \times m$ and $n \times n$, V^T is the common transposition of V , \sum is the $r \times r$ diagonal matrix $r = \min(n, m)$, and its diagonal elements are the nonzero singular values of matrix Y arranged in nonincreasing order, that is, $\lambda_1 \geq \lambda_2 \geq \dots \geq \lambda_r > 0$ represents a matrix of zero elements.

Step 3: Threshold contraction of singular values:

$$\hat{\lambda}_i = \lambda_i - w^*(\lambda_i). \quad (8)$$

Among them $w^*(\lambda_i)$ adaptive threshold, different singular values choose different thresholds to shrink.

Step 4. Use the contracted singular value $\hat{\lambda}_i$ to perform the inverse SVD transformation to obtain an estimate of the matrix Y :

$$\hat{Y} = \begin{pmatrix} \sum & 0 \\ 0 & 0 \end{pmatrix} V', \quad \sum = \text{diag}\{\hat{\lambda}_1, \hat{\lambda}_2, \dots, \hat{\lambda}_r\}. \quad (9)$$

Step 5. Put the denoised small block back to its original position, and average the overlapping pixels.

2.3. Wavelet Analysis Method. Wavelet, that is, a short wave, is a function of fluctuation in a local area. Physically speaking, wavelet has two meanings: "small" and "wave". "Small" means that its definition domain is small, and the range of representation is limited, showing the tight support of the wavelet transform; "wave" means that it has up and down oscillations, that is, the DC component is zero. From a mathematical concept, a wavelet is a function with zero integral [10].

Wavelet analysis analyzes the signal according to the scale and studies the correlation between the signal and the wavelet by expanding and contracting the wavelet. The characteristics of the mathematical microscope are also expressed here: when observing an object at a distance, a large-scale wavelet is used, and its correlation with the signal characterizes the general characteristics of the signal; when observing an object at a close distance, the scale wavelet, its correlation with the signal characterizes the details of the signal.

Definition of continuous wavelet transform: Let $f(t)$ and $\psi(t)$ be square integrable functions and expand the function $f(t)$ under the wavelet basis $\psi(t)$; this expansion is called the continuous wavelet transform of the function $f(t)$, the following is its mathematical expression:

$$CWT_t(a, \tau) \leq f(t), \quad \psi_{a,\tau} \geq \frac{1}{\sqrt{a}} \int_R f(t) \psi^{(t-\tau/a)} dt. \quad (10)$$

Among them, $\psi(t)$ is the wavelet basis function, a is the scale factor, and τ is the translation variable. These two parameters are completed.

The mapping of a time function to a two-dimensional time-scale phase plane.

Discrete wavelet transform discretizes scale factor a and translation variable τ . The current method is to measure the ruler.

The degree a changes by an integer power of 2, namely, $a \in 2^j, j \in \mathbb{Z}$: the translation variable τ is changed in proportion to the integer multiple of a ; that is, $\tau \in \{k2^j, (j, k) \in \mathbb{Z}^2\}$. From this, the expression of discrete wavelet transform is obtained:

$$WT_t(j, k) \leq f(t), \quad \psi_{j,k}(t) \geq \int_R f(t) \hat{\psi}_{j,k}(t) dt. \quad (11)$$

2.4. Image Denoising Based on Wavelet Transform.

Eliminating image noise using the wavelet transform actually belongs to function approximation, a method of properly mapping image space to wavelet function space for better image restoration. The multiresolution characteristics of wavelet transform make the amplitude of the transformed coefficients larger at the edge of the image, and the wavelet transform has a strong correlation between adjacent scale layers, which are conducive to the extraction and protection of image features [11, 12].

Early wavelet denoising methods compare wavelet coefficients based on fixed thresholds, similar to lossy compression techniques, and rely entirely on experience and practical application in the selection of thresholds. With the continuous improvement of theoretical basic knowledge, wavelet denoising methods have also developed rapidly. There are many image denoising and improvement methods based on wavelet transform, but they can be generally divided into three categories: wavelet coefficient threshold shrink denoising, the principle of modulus maximum denoising, and wavelet coefficient correlation denoising.

2.4.1. Wavelet Coefficient Threshold Shrink Denoising.

The wavelet coefficient threshold shrinkage denoising method is simple and easy to implement and has been widely used. After the image undergoes wavelet transform, its signal energy is mainly concentrated on a few wavelet coefficients with larger amplitude, and Gaussian white noise is still white noise after orthogonal wavelet transform, and the amplitude is the same [13]. Therefore, after the wavelet decomposition of the noisy image, the energy of the noise part is mainly concentrated in the high-frequency component, and the distribution is relatively uniform, which is included in the wavelet coefficients with a small amplitude and a large number, while the energy of the image signal is concentrated in a few wavelet coefficients with larger amplitudes. According to this theory, we can roughly take those few

wavelet coefficients with large amplitude as the main signal of the image, while those with uniformly distributed small amplitude are the noise signals. By selecting an appropriate threshold, the coefficient smaller than the threshold is set to 0, and the coefficient larger than the threshold can be retained or changed according to different threshold functions. Finally, through the inverse wavelet transform, the processed wavelet coefficients are converted into image signals, to achieve the purpose of image denoising.

2.4.2. Modulus Maximum Denoising. The singularity of the signal shows that there is a discontinuous point or a certain derivative discontinuity in the signal, which is reflected on the image to indicate the region where the grayscale of the image changes suddenly, and the Lipschitz index is used to describe the regularity and singularity of the signal an important index. The local maximum point of the amplitude of the wavelet coefficient is the mutation point of the image signal, and its Lipschitz index is positive, while the Lipschitz index of the noise signal is negative. Therefore, if the maximum value of the wavelet transform of a singular point decreases with the increase of the wavelet decomposition scale, the Lipschitz index of the singular point is negative, and the point is considered a noise point and it is removed; if the wavelet transform the maximum value of the modulus increases with the increase of the scale of wavelet decomposition, then the Lipschitz exponent of this point is positive, which is regarded as the image signal and retains this point.

Modulus maximum denoising method based on wavelet transform has low dependence on noise and stable performance, which is suitable for signals with low signal-to-noise ratio. However, affected by the calculation accuracy, the denoising effect of this denoising method is not very ideal.

2.4.3. Correlation Denoising Method of Wavelet Coefficients. The wavelet coefficient correlation denoising method distinguishes the signal and noise according to the different propagation characteristics of the image signal and noise in multiscale decomposition. Correlations can be divided into two types: intralayer correlation and interlayer correlation. Intralayer correlation means that under the same scale, the coefficient of the neighborhood with the larger coefficient tends to be larger. Interlayer correlation means that the wavelet transform characteristics of image signals have propagation characteristics at different decomposition scales; that is, when the amplitude of one wavelet coefficient is large, the next decomposition scale is a subcoefficient, and the amplitude is relatively large. However, for noise, the corresponding wavelet coefficients show weak correlation or no correlation. Therefore, you can make full use of the correlation characteristics of the above analysis to distinguish between signal and noise, remove the wavelet coefficients related to noise as much as possible, retain the coefficients corresponding to the image signal, reduce image restoration errors, and achieve better denoising effect.

2.5. Security and Communication Networks. With the extensive application and continuous development of Internet technology, the role of computer networks in modern life has become increasingly prominent and has become one of the future development trends. Individuals, enterprises, government departments, and even national military departments are increasingly relying on the Internet to transmit information. However, the openness and sharing of the network easily make it vulnerable to external attacks and destruction or even paralysis. A variety of intrusions and criminal activities follow one after another, and the security and confidentiality of information are seriously affected. The issue of network security has become one of the most concerned issues of governments, enterprises, and the majority of network users in the world.

Now that computers all over the world will be interconnected through the network, the connotation of information security will also undergo a fundamental change. It has not only changed from general defense to universal defense, but also from a professional field to a public consensus. Network security technology refers to technical means dedicated to solving, such as how to effectively carry out intervention control and how to ensure the security of data transmission, mainly including physical security analysis technology, network structure security analysis technology, system security analysis technology, management security analysis technology, and other security services and security mechanism strategies.

With the rapid development of network technology today, the research on network security technology is of great significance. It is related to the interests of individuals and the security of the country. The research of network security technology is to do our best to create a good network environment for individuals and the country, so that network security technology can better serve the majority of users.

3. Experiments

3.1. Experimental Setup. To develop a new method for crop image denoising, we combined it with wavelet transform on the basis of appropriate improvements to SVD to achieve effective processing of crop noise images.

3.2. Experimental Design. A crop image can be regarded as a two-dimensional matrix, assuming the size of the matrix is $m \times n$ ($m, n \in \mathbb{Z}^*$). Filter the image with low-pass filter A and high-pass filter B, and then sample to achieve wavelet refinement of the image. The high-frequency component of the image wavelet decomposition subimage is represented by B, and the low-frequency component is represented by A. The image is subjected to wavelet decomposition to obtain four subimages with different directions and different resolutions; that is, AA1 is the first layer of low-frequency subimages; BA1 represents the first layer of high-frequency subimages; AB1 represents the first-layer horizontal high-frequency subimages; BB1 represents the first-layer high-frequency diagonal subimage. Performing two-layer wavelet

decomposition on AA1 can obtain AA2, BA2, AB2, and BB2, and continuing to perform three-layer decomposition can similarly obtain AA3, BA3, AB3, and BB3. The theoretically unlimited wavelet decomposition can still be performed for AA3. The image three-layer wavelet decomposition process is shown in Figure 1.

3.3. Experimental Procedure

3.3.1. Adaptive SVD Algorithm in Horizontal (or Vertical) Direction

Step 1 is beneficial to deal with them separately. After the image undergoes singular value decomposition, for the subimages distributed in the horizontal and vertical directions, the image calculates the mean of the above singular value sequence

$$\bar{\lambda} = \frac{1}{\tau} \sum^j \lambda_j. \quad (12)$$

The singular value of the sequence is compared with $\bar{\lambda}$, and the singular value sequence less than $\bar{\lambda}$ is denoted as Q_1 , and the singular value sequence greater than $\bar{\lambda}$ is Q_2 .

Step 2. Since the singular value in the Q_1 sequence is small, the matrix vector corresponding to this singular value does not participate in the reconstruction.

Step 3: Calculate the mean value of singular value $\bar{\lambda}_{Q_2}$ in the sequence Q_1 , record the singular value sequence less than $\bar{\lambda}_{Q_2}$ in the sequence as Q_{11} , and the rest as Q_{12} .

Step 4. Reconstruct the matrix vector corresponding to all singular values in the singular value sequence Q_{12} .

3.3.2. Diagonal Direction Adaptive SVD Algorithm

Step 1: Arrange the singular values in the sequence $\{\lambda'_1, \lambda'_2, \lambda'_3, \dots, \lambda'_j\}$ in order of size, and take the median value $\lambda'_x (x < j)$.

Step 2: The sequence composed of the singular values greater than λ'_x in the sequence $\{\lambda'_1, \lambda'_2, \lambda'_3, \dots, \lambda'_j\}$ is denoted as P_1 , and the sequence composed of the remaining singular values is P_2 .

Step 3: Calculate the mean value of all singular values in the sequence $\{\lambda'_1, \lambda'_2, \lambda'_3, \dots, \lambda'_j\}$:

$$\bar{\lambda}' = \frac{1}{\tau} \sum^j \lambda'_j. \quad (13)$$

Record the sequence composed of the singular values greater than $\bar{\lambda}'$ as Q'_1 and record the sequence composed of the remaining singular values as Q'_2 .

Step 4: Compare the sequence P_1 with Q'_1 , and record the sequence composed of the same singular value in the two sequences as O_1 .

Step 5: Compare the sequence P_2 with Q'_2 , and record the sequence composed of different singular values in the two sequences as O_2 .

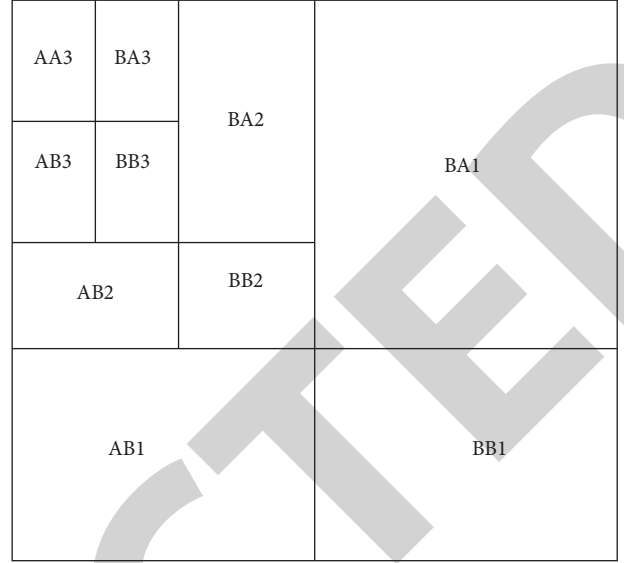


FIGURE 1: Image three-layer tower wavelet decomposition.

In step 6, the singular values represented by O_1 and O_2 and the corresponding matrix vectors are used as the matrix vectors of the diagonal wavelet subimage reconstruction.

3.3.3. Denoising Process. In the first stage, as shown in Figure 2, a similar image block is searched in a search window, and the weight value $\omega_{st1}(N_i, N_j)$ is assigned. After that, the target image block is obtained in the first stage:

$$\bar{x}(N_i) = \sum_{N_j \in S_i} \omega_{st1}(N_i, N_j) y(N_j). \quad (14)$$

Among them, $\bar{x}(N_i)$ and $y(N_j)$, respectively, represent the target image block and the noisy image block.

In the second stage, the weight $\omega_{st2}(i, i^k)$ is defined according to the similarity between the target image block with the center pixel as i and the 8 neighboring image blocks, and finally the image $\hat{x}i$ after denoising is obtained:

$$\omega_{st2}(i, i^k) = \frac{1}{Z(i)} \exp\left(-\frac{\|\bar{x}(N_i) - \bar{x}(N_k)\|_2^2}{h''}\right), \quad (15)$$

$$\hat{x}(i) = \sum_{i \in N_n} \omega_{st2}(i, i^k) \bar{x}(i^k).$$

Among them, i^k represents the pixel corresponding to the pixel i in the target image block $\bar{x}(N^k)$, $\bar{x}(N^k)$ represents the gray value of the pixel i^k , and h'' is the filtering parameter.

4. Discussion

4.1. Analysis of Filtering Algorithm. To be fair, in the filtering process, the pixel blocks and search window sizes of all these filtering algorithms are set to 6×6 and 18×18 , respectively. The specific parameters are as follows.

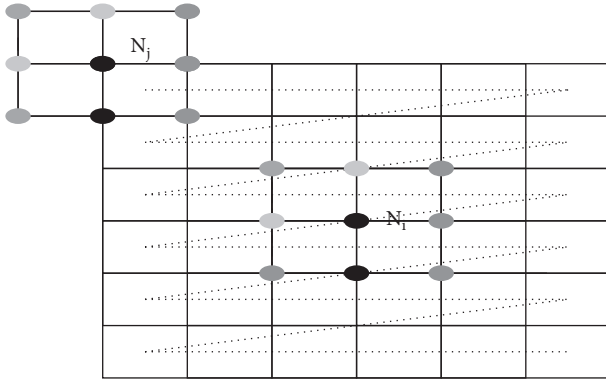


FIGURE 2: The execution process of phase one.

As shown in Table 1, compared with NLM filters, PPB filters have an iterative prior, but their denoising performance is not always better than NLM, when the noise is relatively weak ($\sigma < 30$), the iterative process will make the image detail information blurred, thereby reducing the image quality. For example, in $\sigma = 10$, the PSNR value of the PPB filter is 0.6 dB lower than that of NLM. As the noise increases, the $\Delta\text{PSNR}/\Delta\text{SSIM}$ of PPB becomes larger and larger. When $\sigma > 20$, $\Delta\text{PSNR} = 0.7$ dB. In contrast, whether it is strong or weak, the DNS1 filter is better than PPB and NLM, the only difference between the DNS1 filter and the PPB filter is the a priori term. The former uses one norm, while the latter uses two norms. This shows that the a priori term of the one norm is better for signal retention than the second norm. When $\sigma > 20$, ΔPSNR are higher than other similar algorithms. For example, at $\sigma = 20$, the ΔPSNR of DNS1, DNS2, and DNS3 can reach 1.2 dB, 1.4 dB, and 1.6 dB, respectively. However, when the noise is small, it can be seen that the $\Delta\text{PSNR}/\Delta\text{SSIM}$ of almost all algorithms are not high. It is worth noting that the ΔSSIM value of DNS2 and DNS3 is significantly higher than that of DNS1. Because their priors are the same, this advantage is mainly due to the similarity function S_{n-2} and S_{n-3} can better measure the similarity between noise than S_{n-1} . This is also consistent with the previous analysis conclusions. It should be pointed out that, compared with the NLM filter, the BNLI filter has better denoising performance on House, Cameraman, and Lena data, but slightly worse on Barbara data. This aspect illustrates the superiority of the similarity function S_{n-2} over S_{n-1} . On the other hand, it also shows that the Barbara image contains more details and textures, and the simple noise similarity function S_{n-2} cannot maintain these details well.

4.2. Search Window Analysis. The first stage of the algorithm uses the weighting of all image blocks in the search window to obtain the target image block. To improve the denoising performance, we should search as many similar blocks as possible, so the size of the search window also affects the denoising effect. Most nonlocal denoising methods choose a fixed size search window. Here, we will discuss how the size of the search window affects the denoising performance.

As can be seen from the figure below, the denoising performance of our method increases with the increase of

the search window size and then stabilizes at a window size of about 13×13 . Therefore, generally speaking, a larger search window can provide additional useful information.

When σ increases, we need to choose a larger search area so that we can find more similar pixels, to ensure the denoising ability of the algorithm. According to a large number of experiments, when the noise contains $\sigma = 20, 30, 50$, the best search area order is $11 \times 11, 13 \times 13$, and 21×21 . The best search area is shown in Figure 3.

4.3. Peak Signal-to-Noise Ratio Analysis. To verify the effectiveness of the algorithm, traditional denoising methods such as median filtering, mean filtering, Gaussian filtering, and Wiener filtering were used to denoise red jujube, wheat, and apple agricultural products, and different denoising was analyzed and compared method after denoising.

As shown in Table 2 and Figure 4, the peak signal-to-noise ratio (PSNR) of the image after denoising the red, jujube, wheat, and apple images using various methods, it can be seen that the PSNR value of the image after denoising (red jujube: 70.2158; wheat: 74.1144; apple: 71.5917) is significantly higher than the traditional denoising method, the PSNR value has also increased, especially the wheat image has a large increase in amplitude.

As shown in Figure 5, it can be seen that the dense noise points in figure C have been reduced and replaced by a large number of black spots, and the density of black spots on the surface of the crops in the figure is relatively large, which interferes with the accurate identification. The black dot density in Figure B has been reduced and can be recognized. This shows that it is feasible to perform SVD filtering after rotating the diagonal high-frequency subimage in the SVD wavelet domain to the horizontal or vertical direction.

4.4. Comparative Analysis of Algorithm Running Time. The above are based on the visual effect of the image and the peak signal-to-noise ratio (PSNR) to analyze the performance of the algorithm. Next, the running time of the algorithm will be analyzed and compared, as shown in Figures 6 and 7.

To select different coding lengths, selection rate, hybridization rate, mutation rate, and calculation algebra, the running time histograms of the SVD wavelet domain denoising algorithm are compared. From the figure, it can be seen that the chromosome coding length and calculation algebra pair algorithm are time-consuming and most influential. That is, the smaller the code length, the longer the operation time, the more algebraic operations, and the longer the algorithm running time; the selection rate and hybridization rate have little effect on the time-consuming algorithm, while the mutation rate has almost no effect on the time-consuming algorithm.

5. Discuss

5.1. Improved SVD's Denoising Effect of Crop Image in Wavelet Domain. The threshold improvement algorithm proposed in this paper takes into account the impact of the selection of

TABLE 1: Parameter settings of related filters.

Filter	Similarity function	Parameter settings	Number of iterations
NLM (Sn_1)	SNLM	$h = 6$	—
BNL (Sn_2)	SBNL	—	—
BNL2	SBNL	—	—
Sn_3	Sn_3	$h = 0.6\sigma^2$	—
PPB	SPPB	$\alpha = 0.91, T = 0.3$	24
DNS1	SDNS1	$\alpha = 0.94, \lambda = 0.5\sigma$	6
DNS2	SDNS2	$\alpha = 0.94, \lambda = 0.8\sigma^2$	6
DNS3	SDNS3	$h = 10\sigma^2, \lambda = 10/\sigma$	6

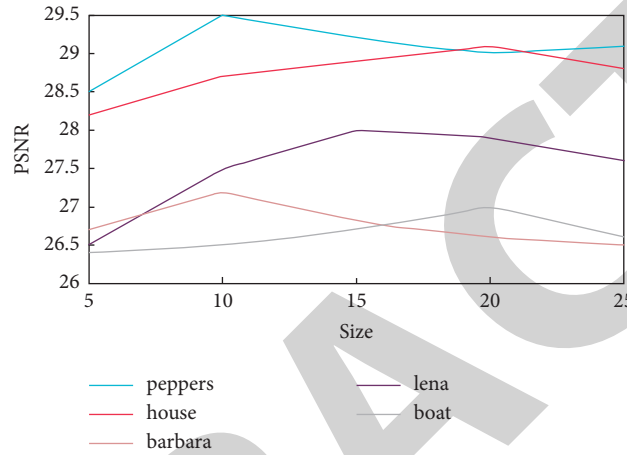


FIGURE 3: Best search area.

TABLE 2: Comparison of PSNR values of images after denoising by various denoising methods.

Denoising algorithm	PSNR (dB)		
	Red dates	Wheat	Apple
Noise image	59.6613	61.2244	61.0021
Gaussian filtering	63.5124	64.5127	63.0147
Median filtering	65.8145	67.1425	68.1598
Wiener filtering	66.5411	68.1422	66.3325
Mean filtering	68.9412	70.1569	68.2544
SVD wavelet domain	70.2546	72.3149	69.8456
Wavelet to wiener	72.6237	74.1512	70.6155
Paternity	69.6522	68.2115	70.1458
Hybrid wavelet algorithm	70.2158	74.1144	71.5917

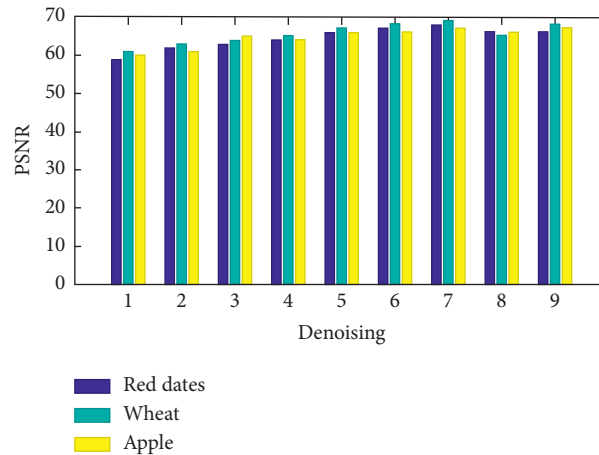


FIGURE 4: Comparison of PSNR values of images after denoising by various denoising methods.



FIGURE 5: (a) Original image, (b) Gaussian noise graph, and (c) salt and pepper noise graph.

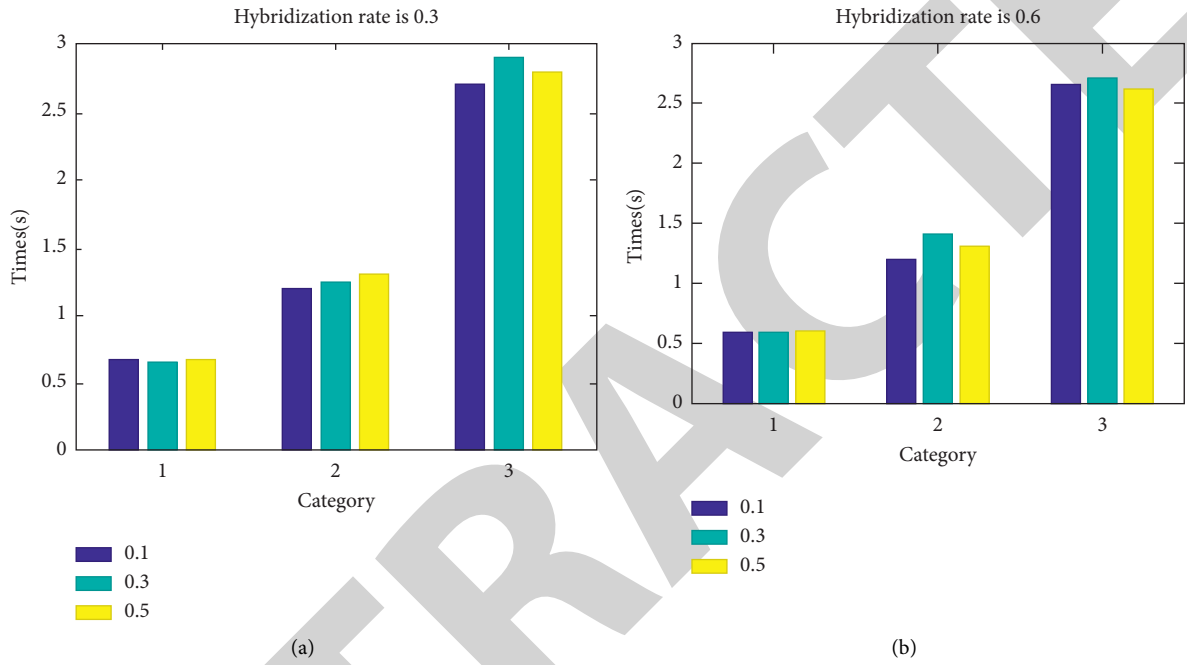


FIGURE 6: Comparison of denoising and time consumption when the encoding length is 4 and the selection rate is 0.6.

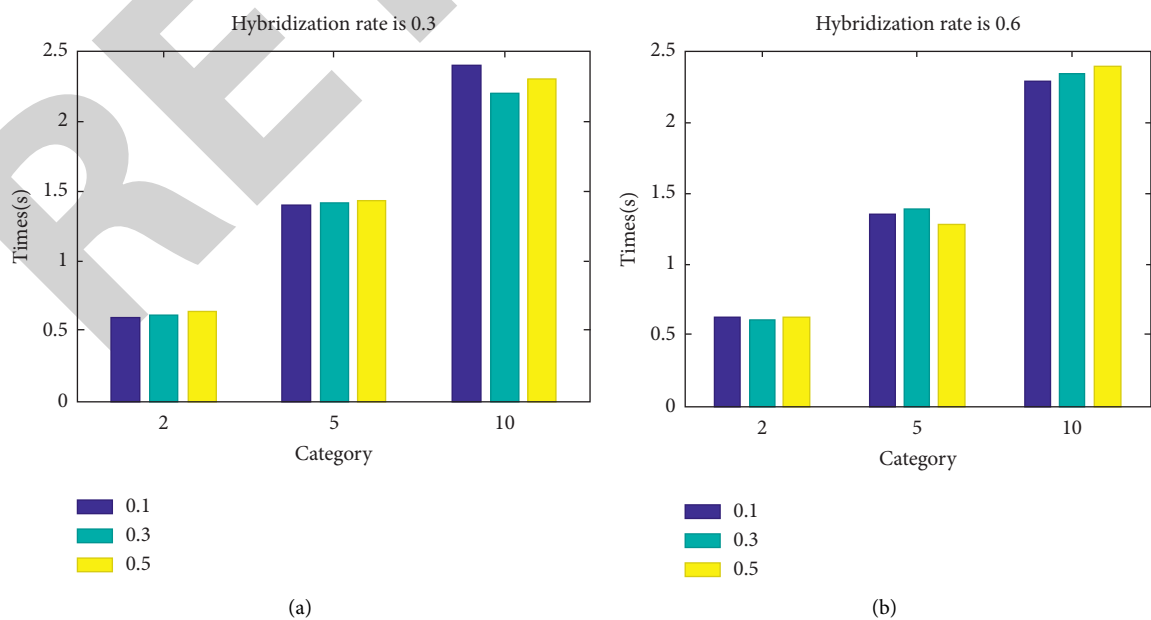


FIGURE 7: Comparison of denoising and time consumption when the encoding length is 8 and the selection rate is 0.9.

the threshold function on the denoising effect and the characteristics of the traditional threshold function that the image is not smooth near the threshold. A new threshold function is designed. The improved threshold function can be very good. The image information is retained to achieve a better denoising effect. The SNR and PSNR obtained are higher than the hard threshold; the soft threshold and the semisoft threshold are higher; and from a visual point of view, the improved SVD wavelet domain cropped image is clearer than the image obtained after denoising. A better denoising effect enables more accurate target detection and recognition as well as tracking and positioning in the follow-up.

5.2. Method Effect Comparison. Comparing different noise reduction methods, it can be seen that the filtering results of the algorithm used in this research can clearly see that there are only a few black spots in the figure, and the image clarity is improved to the maximum extent. This shows that the improvement strategy of this research is better than other, the research is slightly better.

6. Conclusions

In view of the large amount of random noise that often appears in crop images, on the basis of in-depth analysis of the basic principles of the SVD denoising algorithm, combined with wavelet transform, an improved adaptive SVD denoising algorithm in the wavelet domain is proposed. The performance of the algorithm is tested through crop images, and the performance is qualitatively and quantitatively compared with the SVD algorithm and the improved SVD algorithm. The results show that the performance of the algorithm used in this research is slightly better than the other two algorithms, which provides for the processing of crop noise images.

In this paper, the hybrid wavelet transform denoising algorithm has a good visual effect after denoising the agricultural product image; that is, it effectively suppresses the noise in the image and retains the edge details of the image, making the contour of the image after denoising clear and obvious details; compared with traditional denoising methods such as Gaussian filtering, median filtering, Wiener filtering, mean filtering, and wavelet adaptive threshold denoising methods, the peak signal-to-noise ratio of the image after denoising is significantly improved. At the same time, the Lena and Camera images are applied to the hybrid wavelet denoising algorithm. The experimental results show that the hybrid wavelet denoising algorithm not only has good denoising effect and outstanding performance in agricultural product image denoising, but also can obtain a higher the peak signal-to-noise ratio showing that the algorithm is also suitable for general images.

However, since the hybrid wavelet transform algorithm is based on the idea of the basic genetic algorithm, the optimal solution is randomly searched from generation to generation from the initial population, and in the encoding, selection, hybridization and mutation

operations, as the length of the code decreases and the ratio of mixed algebra and selection, hybridization rate, and mutation rate increase, the computational complexity of the algorithm will also increase. In addition, the size of the image matrix is relatively large, which makes the calculation of the algorithm large, and the program running time is relatively long, which cannot meet the needs of real-time processing. This is where the algorithm needs to be improved in the future.

In the proposed double noise similarity (DNS) model, image denoising is transformed into a problem of measuring the similarity of two types of noise. Finally, the two noise similarities are combined in the Bayesian form for image denoising. Compared with other filters based on nonlocal weighted average, this DNS-based algorithm can effectively suppress noise and at the same time maintain good details, but its disadvantage is that the calculation complexity is relatively large.

Data Availability

No data were used support this study.

Conflicts of Interest

The authors declare that they have no conflicts of interest.

References

- [1] J. Jiao, Q. Yang, S. He, S. Gu, W. Rynson, and H. Lau, "Joint image denoising and disparity estimation via stereo structure pca and noise-tolerant cost," *International Journal of Computer Vision*, vol. 124, no. 4, pp. 1-19, 2017.
- [2] L. J. Zhao and F. Cao, "Image denoising algorithm based on composite convolutional neural network," *Moshi Shibie Yu Rengong Zhineng/pattern Recognition & Artificial Intelligence*, vol. 30, no. 2, pp. 97-105, 2017.
- [3] X. Chen, L. Liu, J. Zhang et al., "Infrared image denoising based on the variance-stabilizing transform and the dual-domain filter," *Digital Signal Processing*, vol. 113, no. 1, pp. 103-105, 2021.
- [4] M. Saeedzarandi, H. Nezamabadi-Pour, and A. Jamalizadeh, "Dual-Tree complex wavelet coefficient magnitude modeling using scale mixtures of Rayleigh distribution for image denoising," *Circuits, Systems, and Signal Processing*, vol. 39, no. 6, pp. 2968-2993, 2020.
- [5] J. Q. Vargas, L. R. Khot, R. T. Peters, A. K. Chandel, and B. Molaei, "Low orbiting satellite and small UAS-based high-resolution imagery data to quantify crop lodging: a case study in irrigated spearmint," *IEEE Geoscience and Remote Sensing Letters*, vol. 17, no. 5, pp. 755-759, 2019.
- [6] Q. Dai, X. Cheng, Y. Qiao et al., "Crop leaf disease image super-resolution and identification with dual attention and topology fusion generative adversarial network," *IEEE Access*, vol. 8, pp. 55724-55735, 2020.
- [7] M. Li, R. Idoughi, B. Choudhury, and W. Heidrich, "Statistical model for oct image denoising," *Biomedical Optics Express*, vol. 8, no. 9, pp. 3903-3917, 2017.
- [8] L. Zhuang and J. M. Bioucas-Dias, "Fast hyperspectral image denoising and inpainting based on low-rank and sparse representations," *IEEE Journal of Selected Topics in Applied*

- Earth Observations & Remote Sensing*, vol. 11, no. 3, pp. 730–742, 2018.
- [9] B. Dehda and K. Melkemi, “Image denoising using new wavelet thresholding function,” *Journal of Applied Mathematics and Computational Mechanics*, vol. 16, no. 2, pp. 55–65, 2017.
- [10] C. Brito-Loeza, K. Chen, and V. Uc-Cetina, “Image denoising using the Gaussian curvature of the image surface,” *Numerical Methods for Partial Differential Equations*, vol. 32, no. 3, pp. 1066–1089, 2016.
- [11] J. Yu, L. Tan, S. Zhou, L. Wang, and C. Wang, “Image denoising based on adaptive fractional order anisotropic diffusion,” *Ksii Transactions on Internet & Information Systems*, vol. 11, no. 1, pp. 436–450, 2017.
- [12] V. N. V. S. Prakash, K. S. Prasad, and J. C. Prasad, “Deep learning approach for image denoising and image demosaicing,” *International Journal of Computer Application*, vol. 168, no. 9, pp. 18–26, 2017.
- [13] X. Zhang, “Image denoising using dual-tree complex wavelet transform and wiener filter with modified thresholding,” *Journal of Scientific & Industrial Research*, vol. 75, no. 11, pp. 687–690, 2016.